Photoreduction of 3-Phenylquinoxalin-2-ones by Amines: Transient-Absorption and Semiempirical Quantum-Chemical Studies

Julio R. De la Fuente,* Alvaro Cañete, Claudio Saitz, and Carolina Jullian

Departamento de Química Orgánica y Fisicoquímica, Facultad de Ciencias Químicas y Farmacéuticas, Universidad de Chile, Casilla 233, Santiago 1, Santiago, Chile

Received: November 26, 2001

Photoreduction of 3-phenylquinoxalin-2-ones, XNQ, by triethylamine, TEA, gives a metastable semireduced quinoxalin-2-one via an electron−proton−electron transfer, with unit quantum yields at high amine concentrations. During the photoreduction, an ion-radical pair, $XNQ^{-\bullet}/TEA^{+\bullet}$, a neutral-radical pair, $XNQH^{\bullet}$/TEA-$H^{\bullet}$, and an ion-pair, $XNQH^{-}$/TEA-H^{+}, are formed. We present time-resolved spectroscopic data and quantum mechanical semiempirical AM1, PM3, and ZINDO/S results for the transient species formed during the flash photolysis of quinoxalin-2-ones in the presence of amines. These calculations show that the neutral-radical pair and the ion-pair are similar in energy, and that the calculated spectra of all the transient species should have similar absorption bands near 400 nm in agreement with experimental results. The ZINDO/S calculated spectra of the $XNQH^{-}$/iminium ion pair fit the experimental spectra and explain the lack of visible or near-IR absorption of the metastable compound. Energy changes between the species involved are of interest with regard to the possible use of quinoxalin-2-one/amine systems for light to chemical energy conversion or as temporal data storage devices.

Introduction

Quinoxalin-2-ones and their derivatives have been studied extensively during the last two decades because they are synthetic precursors of antihypertensives and analgesics.[1,2] Other derivatives have been prepared to evaluate their anticancer activity in vitro[3,4] and their use as neurotransmitter antagonists.[5]

Many studies focus on the use of quinoxalin-2-one derivatives as fluorophores for trace analyses of carboxylic acids, alcohols, and amines in high-performance liquid chromatography.[6−10] Quinoxalin-2-ones bound to azacrown-ethers have also been used as fluoroionophores to sense alkali metal ions.[11,12]

Irradiation of substituted 3-phenylquinoxalin-2-ones, in the presence of amines gives the corresponding dihydro-quinoxalin-2-ones, whereas the irradiation of 3-alkyl substituted quinoxalin-2-ones gives the reductive dimers. A mechanism analogous to the photoreduction of ketone triplets by amines has been invoked to explain product formation.[13]

Recently, we reported the thermally reversible photobleaching of 3-phenyl-quinoxalin-2-ones, XNQ, on irradiation in the presence of amines. We proposed a formal hydride transfer mechanism that goes through steps of electron−proton−electron transfer to form the metastable species $XNQH^{-}$ that reverts almost quantitatively in the dark to the initial quinoxalin-2-one.[14]

The processes involved in formation of a metastable semi-reduced quinoxalin-2-one, $XNQH^{-}$, are as follows: photo-excitation of XNQ to its first singlet state, followed by rapid intersystem crossing ($k_{ISC} \approx 10^{10}$ s^{-1}) to generate the triplet state XNQ^{T} with a near unit yield. Then, in the presence of amines of suitable reduction potential, electron transfer takes place giving a triplet ion-radical pair, $XNQ^{-\bullet}/amine^{+\bullet}$. The ion-radical pair can then decay to the starting compound by a back electron transfer, or generate a neutral radical pair via a competitive proton transfer forming the neutral radical pair. We showed that in the presence of triethylamine, TEA, and other hydrogen donating amines, the back electron transfer is inefficient, possibly as the result of a spin forbidden transition.[14]

The neutral radical pair, $XNQH^{\bullet}$/*N*-methylene, formed with hydrogen donating amines such TEA, gives rise by hydrogen abstraction to the reduced 3-phenyl-3,4-dihydro-quinoxalin-2-ones, $XNQH_2$, or to the precursor XNQ or, by a second electron transfer from the *N*-methylene radical, the semireduced metastable species $XNQH^{-}$ can form. From the observed quantum yield of $XNQH^{-}$ ($\Phi_{XNQH^{-}} = 1$), we conclude that this last electron-transfer reaction is far more efficient than the homolytic bond cleavage with transfer of an hydrogen atom.[14] Nevertheless, from the NMR and UV−vis spectra observed for the metastable $XNQH^{-}$, it is difficult to explain the lack of absorption in the visible or near-IR spectrum.[14]

The metastable $XNQH^{-}$ reverts thermally in the dark to the starting 3-phenyl-quinoxalin-2-one, probably by electron transfer from $XNQH^{-}$ to an iminium or an ammonium cation, followed by a back hydrogen atom transfer, in Scheme 1 the overall reaction is shown.

Although the photochemistry of these systems is unusual, similar reversible mechanisms involving electron−proton−electron transfer have been reported for reactions of ketones, quinone derivatives and thioindigo dyes.[15−18] In some of these systems, radical species have been detected by using EPR and/or flash photolysis.

The proposed path of these quinoxalin-2-ones/amine reactions involves several transient species; e.g., an ion−radical pair, a neutral radical pair and an ion pair. In our previous work, attempts to detect radical species by EPR were unsuccessful,[14] but these radical species must appear as intermediates within a solvent cage during formation of $XNQH^{-}$.

The transient species discussed in the preceding paragraphs, possibly show distinctive absorption spectra and evolve kineti-

* To whom correspondence should be addressed. Fax: 56-2-678 2868. E-mail: jrfuente@ciq.uchile.cl.

10.1021/jp014317c CCC: $22.00
Published on Web 07/12/2002

SCHEME 1

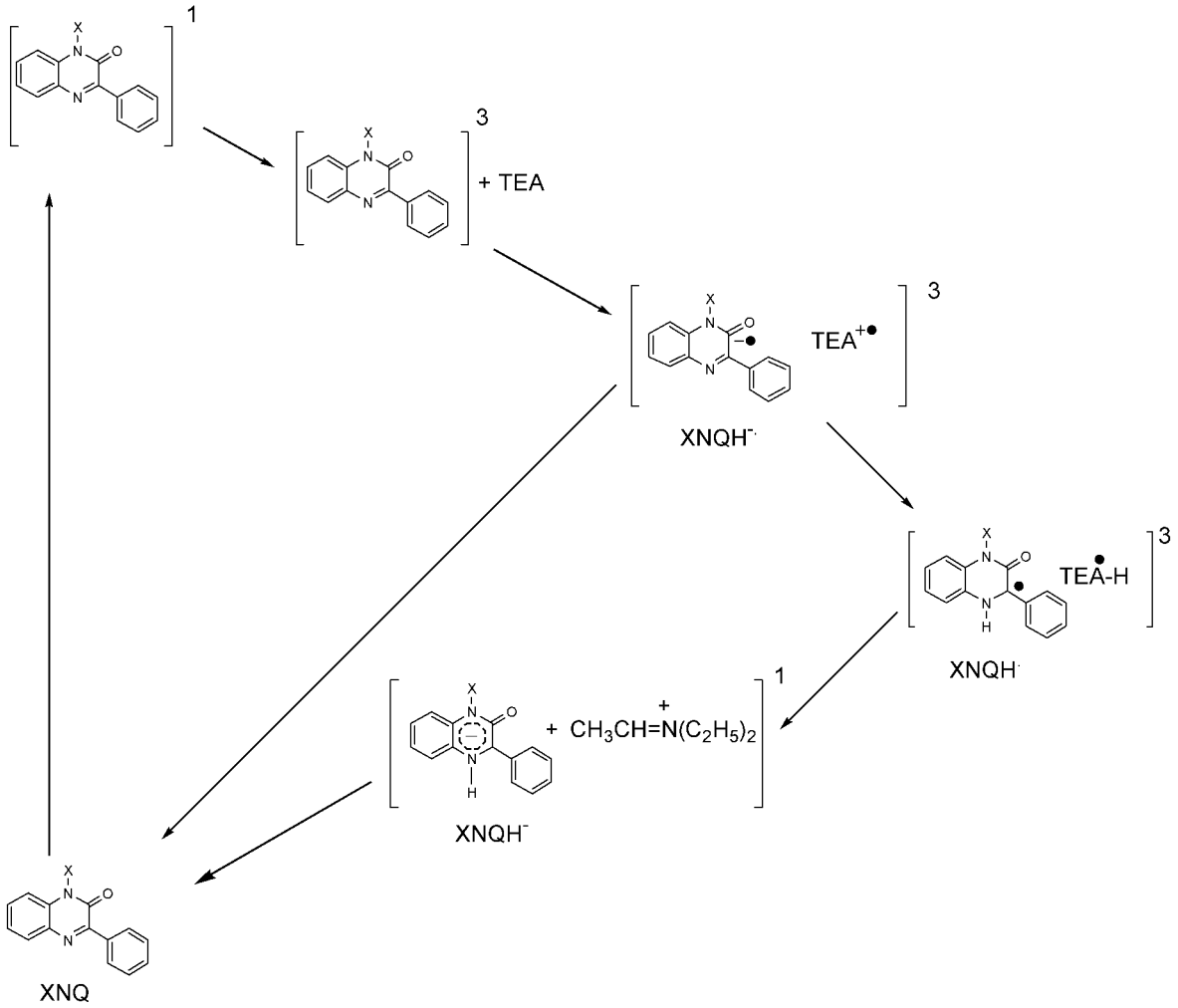

cally on different time scales, thus allowing their detection by flash photolysis. Also, the energy changes between the species involved are of interest as regards the possible use of quinoxalin-2-one/amine systems for light to chemical energy conversion or as temporal data storage devices.[18−20]

In this work, we present experimental time-resolved spectroscopic data and quantum mechanical semiempirical AM1, PM3, and ZINDO/S treatments of the transient species formed during the flash photolysis of quinoxalin-2-ones in the presence of amines.

The molecular mechanical and semiempirical quantum mechanical methods indicate that the neutral radical pair and the ion pair are similar in energy, and that the calculated spectra of all the transient species should have similar absorption bands near 400 nm. Semiempirical calculations also show that the conformation of the ion pair resembles that of the dihydrogenated quinoxalin-2-one $MeNQH_2$, with a pyramidal conformation on C3.

The ZINDO/S calculated spectra of the $XNQH^-$/iminium ion pair fits the experimental spectra of the metastable compound and explains the lack of visible or near-IR absorption for these species.

Results and Discussion

The transient absorption spectra of both quinoxalin-2-ones, HNQ and MeNQ, in nitrogen purged solvents, show a broad band between 350 and 450 nm with maxima at 390 nm. Neither of the quinoxalin-2-ones studied shows ground-state depletion in the overlapped spectral range, probably due to a very large extinction coefficient of the transient species as compared to that of the ground state.

These absorptions have monoexponential decays with lifetimes of about 30 μs, signals that disappear in oxygenated solutions, depending on the concentration of quinoxalin-2-one and the solvent. These absorptions can be clearly assigned to the triplet excited species. The spectra, Figure 1, are similar in acetonitrile or methanol. When *n*-hexane is used as solvent, the transient spectra show some structure with shoulders at 405 and 425 nm. For MeNQ, a triplet quantum yield $\Phi^T = 1.06 \pm 0.18$ was measured by energy transfer to β-carotene, as explained in the Experimental Section. This value agrees with the limiting value previously estimated,[14] and fits the measured fluorescence quantum yield of 0.025 reported therein.

In the presence of amines, spectral changes occur with a slight red shift in the main absorption band, concomitant with the change in decay profiles from monoexponential to multiexponential with a long-lived residual absorption that remains when amine concentrations are increased.

In the presence of triphenylamine, TPA, a shoulder appears in the main band near the maximum and a new absorption is centered at 640 nm.

Quenching experiments, conducted under monoexponential decay conditions, (low amine concentration) were performed with TEA. These experiments showed the expected Stern−

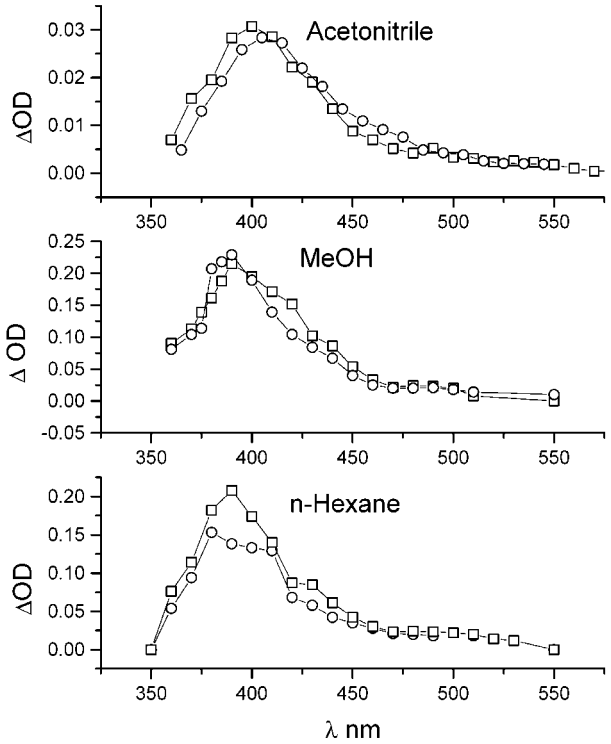

Figure 1. Triplet transient absorption spectra, 2 μs after the laser pulse, for MeNQ (circles) and HNQ (squares) in acetonitrile, methanol and *n*-hexane.

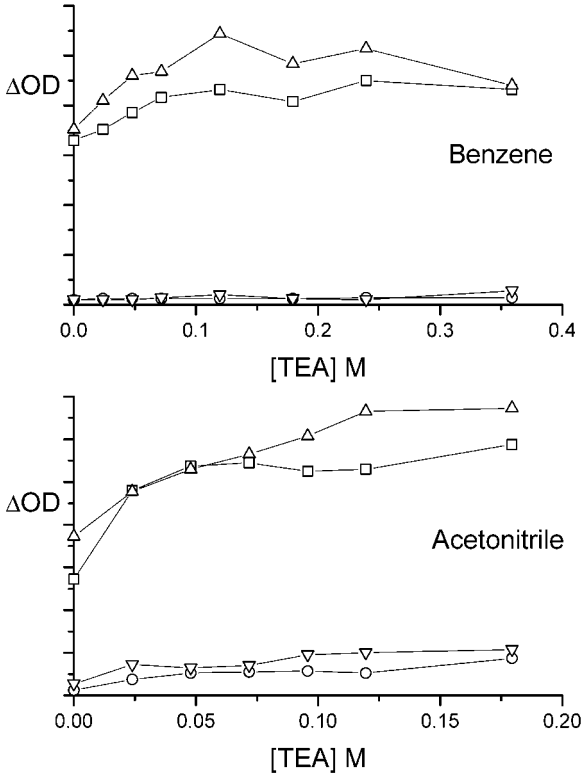

Figure 2. Absorption at 410 nm extrapolated to $t = 0$ and residual absorption v/s TEA concentration, (squares and circles respectively) for the MeNQ/TEA and (up triangle and down triangle respectively) HNQ/TEA systems in acetonitrile and benzene.

Volmer kinetics and at higher [TEA] a multiexponential decay with the enhancement of absorption at the spectral maxima. The increase of extrapolated absorption at $t = 0$, ΔOD_0, related to the absorption in absence of amine, is about 90% in acetonitrile and almost 65% in benzene for both quinoxalin-2-ones, as shown in Figure 2. Also the long-lived, lifetime ca. 300 μs, residual absorption grows with [TEA] up to a plateau. Both of these observations, the increasing absorption and the residual absorption, fit the presence of two or more species absorbing at similar wavelengths. Although the lifetimes of these species could be very different their spectra are quite similar and cannot be resolved by our equipment.

Triplet quenching rate constants were obtained from a Stern−Volmer treatment of lifetime data obtained by the monoexponential fit of decay curves at amine concentration where the decay was monoexponential.

For quenching by TEA in acetonitrile, values of k_q of 4.6×10^6 and 8.2×10^5 $M^{-1}s^1$ were observed for MeNQ and HNQ triplets, respectively. In benzene, values of k_q were 2.0×10^5 and 3.0×10^5 $M^{-1}s^1$ for the same triplet states.

The increase of TEA k_q (23-fold for MeNQ and 2.7-fold for HNQ) from benzene to acetonitrile as solvents can be attributed to existence of a stabilized polar transition state for electron-transfer quenching or to an intermediate charge-transfer complex.

We have previously reported that HNQ forms ground and excited-state complexes with amines,[14] thus an electron-transfer quench of a triplet exciplex by amines cannot be disregarded for any of the quinoxalin-2-ones.

When non-hydrogen donating amines such as 2,2−6,6-tetramethylpiperidine, TMP or triphenylamine, TPA, in acetonitrile, were used as quenchers of $MeNQ^T$, quenching constants were 5.3×10^6 and 5.9×10^7 $M^{-1}s^{-1}$, respectively. For HNQ^T, quenching by TMP has $k_q = 5.7 \times 10^5$ $M^{-1}s^{-1}$.

The k_q values found for $MeNQ^T$ quenched by TEA, TMP, and TPA, shows the expected dependence on the oxidation potentials of the respective amines for an electron-transfer quenching.[21,22]

Although few examples of electron-transfer rates in the range reported here can be found in the literature,[23,24] the low values of k_q reported could be explained by assuming a solvent Marcus reorganization energy of about 4−6 kcal/mol, probably due to the reorientation of dipolar moment vectors in the electron-transfer step.[25,26]

Flash photolysis of MeNQ in the presence of excess TPA showed the characteristic absorption of the triphenylamine cation radical, $TPA^{+\bullet}$, near 640 nm, and a broad band with a maximum at 400 nm and a shoulder at 410 nm, (Figure 3). Aromatic amines are known for their ability to form exciplexes,[27−29] thus absorption due to an exciplex with a considerable character of a charge-transfer complex cannot be disregarded.

From ΔOD at 400 and 650 nm the extinction coefficient for the ion radical pair can be estimated. Taking the reported $\epsilon = 1.3 \times 10^4$ $M^{-1}cm^{-1}$, at 647 nm, for the triphenylamine cation radical[30] and assuming a stoichiometric relationship between the ion radical species, $\epsilon \cong 1 \times 10^5$ $M^{-1}cm^{-1}$ at 400 nm can be estimated for the $MeNQ^{-\bullet}/TPA^{+\bullet}$ transient species. Although this value may be overestimated due to diffusion out of the solvent cage, it is 1 order of magnitude greater than that of the ground-state absorption at 360 nm,[14] and could explain the nondepletion of ground-state absorption by a compensation of the ground-state depletion and the triplet−triplet absorption.

To obtain a spectrum of the individual anion radical, $MeNQ^{-\bullet}$, flash photolysis were carried out by using excess TMP or DABCO. With these non-hydrogen donating amines transient absorptions appear with maxima at 400 and 425 nm for TMP and DABCO respectively, Figure 3. These bands that can be

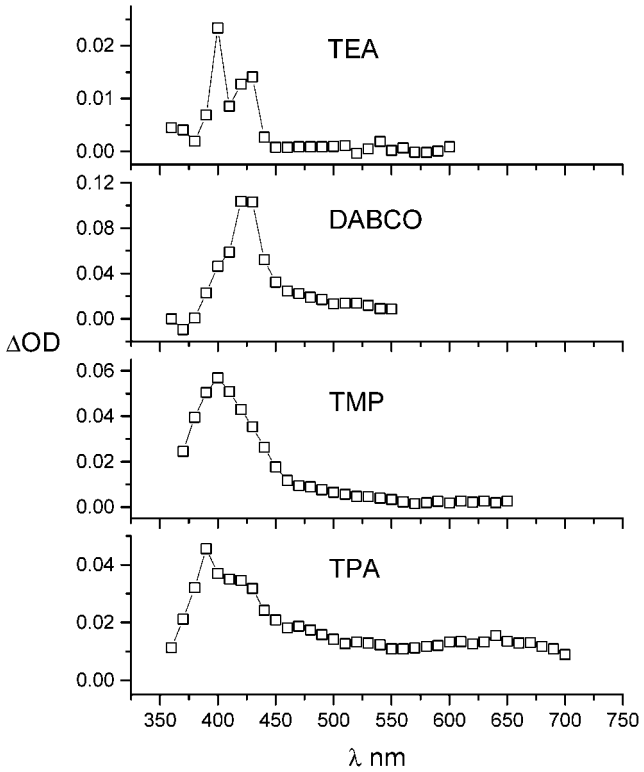

Figure 3. Transient absorption spectra 5 μs after laser excitation at 355 nm, for MeNQ/amine with excess TEA, DABCO, TMP, or TPA in acetonitrile.

assigned to $MeNQ^{-\bullet}$ show a shift of 25 nm for the $MeNQ^{-\bullet}$/$DABCO^{+\bullet}$ system relative to the $MeNQ^{-\bullet}$/$TPM^{+\bullet}$ system. The shifted maxima suggest that there is a strong interaction between a quinoxalin-2-one anion radical and the respective amine cation radical, but in these cases, no further reactions are possible due to the lack of a transferable α-hydrogen. The lifetimes of 25 and 16 μs for the named $MeNQ^{-\bullet}$/$TMP^{+\bullet}$ and $MeNQ^{-\bullet}$/$DABCO^{+\bullet}$ ion radical pairs can be related to back electron transfers from the paired ion radicals with k_{-ET} of 4.0×10^4 and 6.3×10^4 s^{-1} respectively. For the system $MeNQ^{-\bullet}$/$TPA^{+\bullet}$, a back electron-transfer rate constant of 4.7×10^4 s^{-1} was estimated from decay times of absorptions at 400 and 650 nm. These results are consistent with the low estimated rate constant for the back electron-transfer processes and fit a spin forbidden electron retrotransference.[14]

Figure 3 also includes the spectrum obtained for MeNQ with a large excess of TEA. It shows clearly two absorptions bands that we can assign to the transient ion-radical pair $MeNQ^{-\bullet}$/$TEA^{+\bullet}$, and to the transient neutral radical pair $MeNQH^{\bullet}$/$TEA\text{-}H^{\bullet}$.

Previously, we estimated a limiting value of 1.0 for the quantum yield of the metastable photoproduct Φ_{XNQH^-} that is given by the following equation[14]

$$\Phi_{XNQH^-} = \frac{\Phi^T k_{ET} k_{H^+} k_q[\text{amine}]}{(k_{-H} + k_{ET})(k_{-ET} + k_{H^+})(k_d{}^T + k_q[\text{amine}])}$$

where Φ^T is the triplet quantum yield with unit value; k_{ET} is the rate constant for the second thermal electron transfer that is much more efficient than the proton retro-transfer rate, k_{-H}, that involves the hydrogen atom transfer from the neutral radical $XNQH^{\bullet}$ to the iminium radical, with the homolytic breakdown of a N−H bond and the spin-flip of an electron. The proton-transfer rate constant, k_{H^+}, from the $TEA^{+\bullet}$ radical cation, that follows the photoinduced electron transfer, has been estimated to occur in the picosecond time scale in similar systems.[15−17,31] The electron-transfer quenching rate constant by TEA, k_q, is in the order 10^6 $M^{-1}s^{-1}$. The back electron-transfer rate constant that describes deactivation of the ion-radical pair, k_{-ET}, (∼) 5×10^4 s^{-1} and the triplet decay rate constant, $k_d{}^T$ (∼) 3×10^4 s^{-1}, replacement by these values in the Φ_{XNQH^-} equation gives a limiting value of 1.0 at high concentration of amine.

Then, the limiting value of 1.0 for the efficiency of the metastable photoproduct formation fits with the inefficient electron retro-transfer as compared to proton transfer and to a near complete interception of XNQ^T by the corresponding amine.

Semiempirical Quantum Calculations

Semiempirical molecular orbital calculations AM1[32] and PM3,[33] (HyperChem 6.0 software) were performed to estimate geometries and heats of formation of the molecules and molecular systems involved in the proposed reactions.

Calculations were made for single molecules, radicals and the ion of XNQ and also over the entire molecular system, XNQ/TEA, considering the respective ion-radical pairs, radical pair and ion pair, using the restricted Hartree−Fock method, RHF, for either open or closed shell systems.

Semiempirical methods used here provide rapid results, which although unlikely to be quantitative, give useful qualitative information, especially when relative energies are compared. Although the RHF method is not the most appropriate for energy calculations of open shell systems, the approximation has been used successfully for calculations of neutral molecules, cation-radicals and dications of carotenoids[34] and butadiene derivatives.[35] However, the following energy calculations were made disregarding solvent stabilization energies of charged species. Thus, the energies reported below are useful only comparatively.

The procedure was as follows. For a single molecule, the geometry was first optimized by using MM+ molecular mechanics[36] followed by unrestricted geometrical optimization at the semiempirical levels, AM1 and PM3.

Electronic energy calculations were performed on the optimized neutral molecules XNQ, for the ground, S_0, and first excited electronic states, singlet S_1 and triplet T_1 by using the ground state optimized geometry. To obtain a geometry for the relaxed first excited triplet state a new optimization was made, but now setting the multiplicity of the lowest excited state to 3. This last, geometrically relaxed, triplet was used for the next calculations.

The anion radical $MeNQ^{-\bullet}$ was generated by setting the proper charge and multiplicity to the relaxed triplet T_1 geometry, and optimized to obtain the geometry and heat of formation.

The neutral radical, $MeNQH^{\bullet}$, was generated by adding a hydrogen to the N 4 atom of the optimized structure of $MeNQ^{-\bullet}$, setting the proper multiplicity and charge, and then performing the unrestricted geometrical optimization. From an optimized geometry, we also obtained the respective heat of formation. To generate the semireduced species, $MeNQH^-$, the optimization was performed for the neutral hydrogenated radical $MeNQH^{\bullet}$ by setting the proper multiplicity and charge.

With optimized geometries of each of the species mentioned in the preceding paragraphs, electronic spectra were calculated by ZINDO/S,[37,38] optimized specifically for spectroscopy.

The calculated spectra were obtained with the restricted Hartree−Fock configuration interaction, with orbital criteria using the first 5 unoccupied and 5 occupied MO and the proper multiplicity and weighting overlap factors values of 1.267 and

TABLE 1: Calculated Spectra for Transient Species in Quinoxalin-2-one Photoreduction by TEA

	MeNQ		HNQ	
	AM1	ZINDO/S[a]	AM1	ZINDO/S[b]
species	λ nm (osc. strength)	λ nm (osc. strength)	λ nm (osc. strength)	λ nm (osc. trength)
XNQ	353.1 (0.290)	347.0 (0.214)	352.1 (0.301)	343.8 (0.407)
		337.8 (0.465)		336.8 (0.287)
	287.3 (0.126)	292.9 (0.168)	287.8 (0.119)	293.0 (0.171)
XNQ^3		676.4 (0.162)	543.4 (0.120)	496.5 (0.115)
	467.1 (0.146)	462.4 (0.138)		
	381.9 (0.773)	382.3 (0.142)	394.1 (0.292)	409.6 (0.514)
			273.0 (0.258)	
			258.7 (0.226)	210.1 (0.584)
$XNQ^{-\bullet}$			423.5 (0.276)	
	411.6 (0.557)	409.4 (0.727)	398.1 (0.299)	409.9 (0.759)
	394.1 (0.321)	381.1 (0.175)	388.4 (0.297)	378.7 (0.133)
$XNQH^{\bullet}$				357.0 (0.120)
				284.2 (0.248)
	448.7 (0.407)	420.4 (0.152)	448.5 (0.391)	413.5 (0.168)
$XNQH^-$	381.6 (0.244)	369.0 (0.470)	381.9 (0.291)	360.5 (0.513)
			291.8 (0.105)	
	253.6 (0.285)	266.6 (0.115)	267.2 (0.101)	264.5 (0.140)

[a] Calculated with AM1 optimized geometry [b] Calculated with PM3 optimized geometry.

0.585 were used for $\sigma-\sigma$ and $\pi\pi$ overlap respectively.[39] Although high gradient values (190 kcal/Å mol) were obtained with the AM1 and PM3 geometries in the CI calculations with ZINDO/S, the spectra so obtained were similar to those obtained by using CI with AM1 or PM3.

The more relevant spectroscopically active transitions (oscillator-strength > 0.1) calculated for the molecular species are summarized in Table 1. Although calculations are for a vacuum, with the optimized AM1 or PM3 geometry and using ZINDO/S, all the calculated spectra show active absorptions compatible with the transient spectra.

The fit between experimental and calculated transient spectra can be attributed to low changes in the dipolar momentum of the states involved, disregarding large solvent Stokes shifts.[40]

The calculated spectra for the hydrogenated anion $XNQH^-$ indicate conservation of the band at 360 nm for both quinoxalin-2-ones and appearance of new absorption bands at 413 and 420 nm for X = H- and Me- respectively. But the metastable $XNQH^-$ does not show an absorption near 400 nm and moreover bleaching of XNQ was followed by disappearance of the bands at 360 nm.[14]

However, the calculations discussed earlier were made with only one of the species involved excluding TEA and their radicals. To have a more realistic view of the reaction path, calculations were made over the entire molecular system.

Optimizations of the molecular systems were made, first by a fully separated optimization of the quinoxalin-2-one, XNQ, and TEA at AM1 and PM3 levels, then both molecules were merged and fully optimized as a molecular system.

Several optimizations with different initial locations for the amino nitrogen of TEA with respect to the quinoxalin-2-one were made to find the most stable conformation for the molecular system. The TEA nitrogen was put close to N 1, N 4 atoms and close to the C=O bond of quinoxalin-2-one. For all of these optimizations of TEA with MeNQ, geometries converge to those shown in Figure 4-a, 4-b, regardless of different torsional angles between the heterocyclic ring and phenyl of 39.1° and 61.4° for AM1 and PM3 geometries, respectively. The differences in torsional angles can be attributed

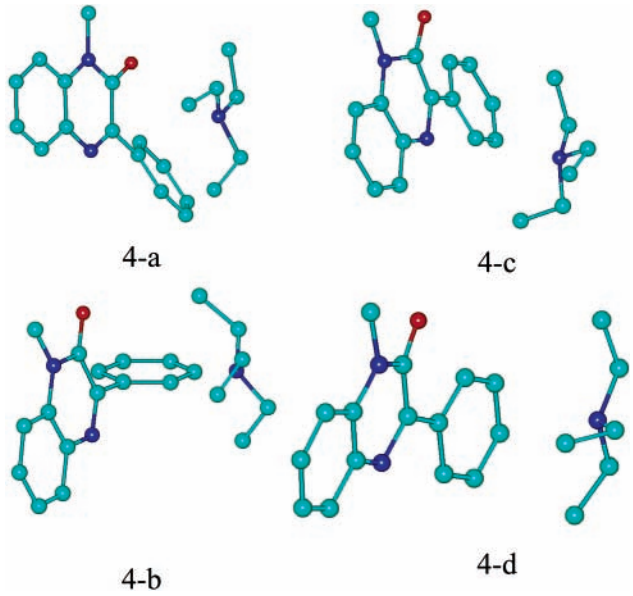

Figure 4. Geometries for (a) AM1 MeNQ/TEA ground state, (b) PM3 MeNQ/TEA ground state, (c) PM3 relaxed triplet state $(MeNQ/TEA)^3$, and (d) PM3 triplet ion-radical pair $(MeNQ^{+\bullet}/TEA^{-\bullet})^3$

to the different parameter sets used in both methods. Nevertheless, the AM1 and PM3 configurations converge.

From this ground-state optimized geometry, levels of the first singlet and triplet excited states were calculated, and that of a relaxed excited triplet state was also calculated by optimization of the former triplet state system. Almost identical geometries were obtained with both AM1 and PM3. Figure 4-c shows the PM3 optimized relaxed $(MeNQ/TEA)^3$ system.

By using the relaxed triplet state geometry of the molecular system, the ion−radical pair was generated by setting the charge of each molecule of the system to its appropriate value, followed by a full geometrical optimization of the whole system with triplet multiplicity. The PM3 optimized geometry for the triplet ion-radical pair is shown in Figure 4-d.

Optimization performed by using singlet multiplicity, irrespective of the method used, leads to a geometry and energy close to those of the ground-state, in agreement with rapid back electron transfer.

The neutral radical pair was built by adding a hydrogen to the N 4 atom of quinoxalin-2-one and deleting the neighboring hydrogen from the α-C of TEA. Then the geometrical optimization of the system was made with triplet and singlet multiplicities. As expected, the lower energy state is the triplet with the related singlet being higher in energy by ca. 47 and 20 kcal/mol, calculated by using AM1 or PM3, respectively.

Figure 5-a shows the PM3 geometry triplet radical pair (AM1 geometry was almost identical), displaying the hydrogen atoms.

The singlet state for the neutral radical pair converges to a system with charge-transfer character, calculated by either AM1 or PM3, with loss of biradical character. Thus, we can disregard spin-flip induced by proton transfer. These results support our previous assumption that reaction proceeds along the triplet surface with species confined in the solvent cage.[14]

Using the optimized neutral radical pair with geometry of the triplet, and setting the proper charges to $MeNQH^-$ and $TEA\text{-}H^+$ a new optimization was performed considering both singlet and triplet multiplicity. Nevertheless, the triplet states of $MeNQH^{\bullet}/TEA\text{-}H^{\bullet}$ and $MeNQH^-/TEA\text{-}H^+$ where almost isoenergetic calculated by using either AM1 or PM3, and would be

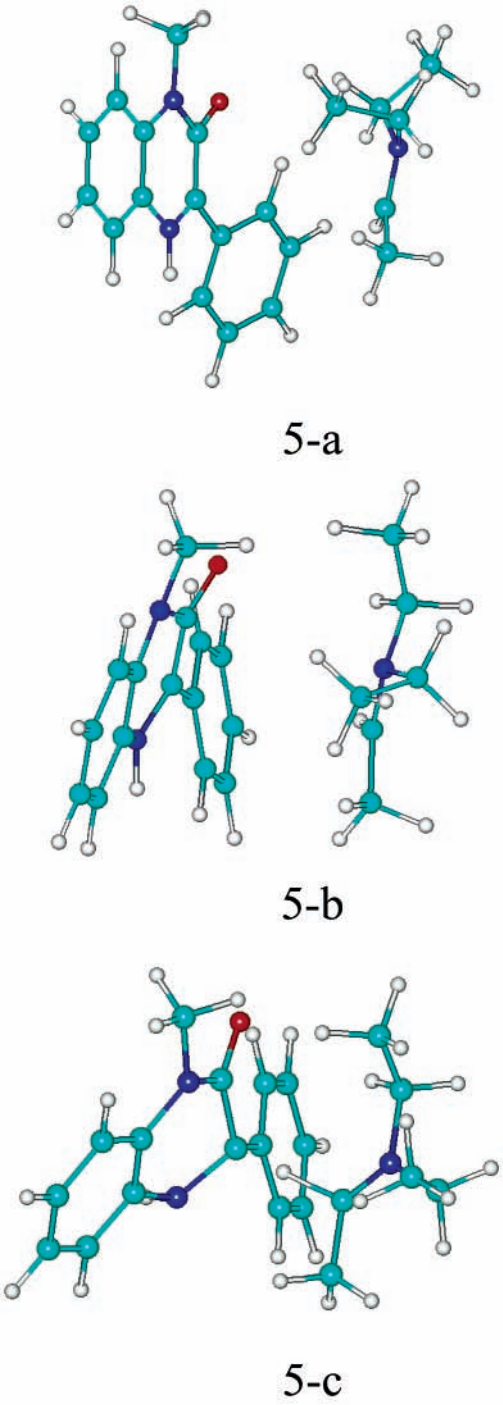

Figure 5. Geometries for (a) PM3 triplet radical pair (MeNQH•/TEA-H•)[3], (b) PM3 triplet ion-pair (MeNQH$^-$/TEA-H$^+$)[3], and (b) PM3 singlet ion-pair(MeNQH$^-$/TEA-H$^+$)[1]. The PM3 singlet ion-pair is only 5 kcal/mol above the PM3 triplet radical pair and their predicted ZINDO/S spectra do not show active transitions above 300 nm.

reached easily in the second thermal electron transfer, in agreement with the proposed equilibrium between these species.[14]

Figure 5-b and 5-c, shows the PM3 geometries for the triplet ion-pair and the singlet ion-pair, respectively. Those obtained by using AM1 were very similar and are not shown.

For the system MeNQH$^-$/TEA-H$^+$, the singlet state energy calculated by the PM3 method is only 6 kcal/mol over that of the respective triplet. These results suggest that the ground states for the ion-pair formed in the second thermal electron transfer probably have singlet multiplicity.

Despite the approximations used for the energy calculations in the preceding paragraphs, the results show a downhill progression of stored energy from the triplet system to the ion-pair system. Calculations made by using UHF for the relaxed triplet (MeNQ/TEA)[3] and ion-radical pair (MeNQ$^{-\bullet}$/TEA$^{+\bullet}$)[3] show an uphill electron transfer step with a change of enthalpy of 32 kcal/mol, calculated at PM3 levels, with the UHF ion-radical pair only 7 kcal/mol above to those of RHF. These results prevent our using UHF methods that probably underestimate the triplet system energy.

To have a more realistic model of absorptions of transient species generated in the reaction path, spectra were calculated for the most stable geometries of the lowest energy states for each transient species. In using ZINDO/S, with the proper multiplicity and using restricted Hartree−Fock CI with the orbital criteria, we took the first 5 unoccupied and 5 occupied MO of the predicted AM1 and PM3 most stable conformations. The results of these calculations are summarized in Table 2, where only spectroscopically active transitions (with oscillator strength > 0.1) and wavelengths >250 nm are considered.

These results in Table 2 are well fitted to the experimental spectra of ground and transient species. For triplet MeNQ/TEA the ZINDO/S more intense absorption is predicted to appear at 407 nm with AM1 and at 461 nm with PM3 predicted geometries.

For the ion-radical pair triplet state, the most intense calculated absorptions were at 404 and 458 nm for AM1 and at 400 and 440 nm for PM3 geometries. These predicted wavelengths fit closely the experimental transient spectra shown in Figure 3, although respective intensities do not fit calculated oscillator forces, possibly due to a simultaneous contributing absorption of an hydrogenated neutral radical pair near 380 nm.

For the neutral triplet state of the radical pair, the higher absorption appears at 384 nm and 376 nm for AM1 and PM3 geometries, respectively. Calculation predicts that the triplet state ion-pair should have the highest absorption near 380 nm but, experiment shows no absorption above 300 nm. In agreement with experiment, the triplet state appears to be energetically disfavored. However, the singlet state calculated spectrum should not show absorption over 250 nm and this state is energetically feasible.

Both AM1 and PM3 methods qualitatively fit results with respect to energies of species involved. The inability of AM1 to predict the spectrum of the metastable ion-pair and the agreement between experimental and calculated ZINDO/S spectra for the optimized PM3 geometry, permit us to conclude that PM3 optimized geometries give a better representation of the molecular systems studied.

PM3 differs from AM1 only in values of the parameter set, mainly at the core−core repulsion functions that overestimate the nuclear−nuclear repulsion terms in AM1 in contrast to PM3 where non bonded interactions are less repulsive than in AM1. Also, the fully optimized parameter sets used in PM3 were derived by comparing a larger and wider variety of experimental versus computed molecular properties.[39]

Conclusions

The calculations, together with the energetic considerations, lead us to conclude that the reaction path involves the triplet surface of the molecular system, with a resulting singlet ion-pair, possibly attained by spin-flip during the second thermal electron transfer.

The MeNQ/TEA system energy storage capacity, calculated as the ratio between stored and absorbed energy, can be

TABLE 2: Calculated Spectra for Transient Molecular Systems in the Photoreduction of Quinoxalin-2-one by TEA

	AM1	ZINDO/S[a]	PM3	ZINDO/S[b]
molecular system	λ nm (osc. strength)	λ nm (osc. strength)	λ nm (osc. strength)	λ nm (osc. strength)
MeNQ/TEA	351.3 (0.302) 288.1 (0.137) 257.7 (1.122)	341.5 (0.699) 293.8 (0.154) 241.9 (0.289)	341.1 (0.139) 271.1 (0.087) 261.5 (0.978)	319.7 (0.456) 277.7 (0.170)
$[MeNQ/TEA]^3$	534.7 (0.236) 432.6 (0.230)	456.1 (0.294) 407.1 (0.374)	509.0 (0.234) 446.7 (0.136) 428.3 (0.157) 322.8 (0.113) 273.1 (0.132)	672.3 (0.114) 461.0 (0.217) 381.4 (0.116)
$[MeNQ^{-\bullet}/TEA^{+\bullet}]^3$	541.0 (0.271) 432.3 (0.133) 418.0 (0.112) 270.8 (0.168)	458.0 (0.262) 403.5 (0.406)	514.8 (0.266) 429.3 (0.213) 321.2 (0.104) 272.8 (0.164)	439.8 (0.312) 399.9 (0.332)
$[MeNQH^{\bullet}/TEA\text{-}H^{\bullet}]^3$	387.1 (0.464) 262.5 (0.130) 260.8 (0.221) 250.2 (0.294)	384.4 (0.225) 312.8 (0.141) 283.4 (0.115)	386.6 (0.330) 339.9 (0.144) 276.5 (0.232) 254.4 (0.226)	375.9 (0.275) 283.1 (0.138)
$[MeNQH^{-}/TEA\text{-}H^{+}]^3$	389.5 (0.451) 259.9 (0.282) 250.1 (0.266)	382.3 (0.209) 357.4 (0.134) 310.5 (0.104) 282.8 (0.112)	417.5 (0.138) 388.2 (0.254)	374.3 (0.238)
$[MeNQH^{-}/TEA\text{-}H^{+}]^1$	397.0 (0.272) 365.3 (0.312)	*c*	253.9 (0.997)	248.4 (0.178) 236.3 (0.214) 204.7 (0.582)

[a] Calculated with AM1 optimized geometries. [b] Calculated with PM3 optimized geometries. [c] Negative frequencies.

estimated as 44% from AM1, and 36% from PM3 values, considering the more probable singlet ion-pair with a strong interaction between the pyramidal C-3 of quinoxalin-2-one and the α-H of the iminium anion. These estimations neglect solvation energies of the involved species.

The long persistence of the ion-pair and the energy storage capacity results indicate possible technological applications in temporal digital data storage devices or solar energy to chemical energy conversions.

Experimental Section

Acetonitrile, hexane, methanol, and benzene were Merck HPLC or spectroscopic grade and were used as received.

Triethylamine, Aldrich, was stored over potassium hydroxide prior to vacuum distillation trap-to-trap, and 2,2,6,6-tetramethylpiperidine, Aldrich 99 + % was also vacuum distilled. Both amines were sealed into glass tubes at 10^{-4} Hg mm and stored at −18 °C. Before each experiment a new tube was opened to ensure freshness of the amine.

DABCO, Aldrich, was used as received. DABCO solutions were prepared immediately before use. Triphenylamine, Aldrich 98% was purified by re-crystallization from methanol.

(1,4)Quinoxalin-2-ones. (1,4)Quinoxalin-2-ones were prepared from the required *o*-phenylendiamine and methyl benzoylformate, in THF/pyridine[13] (10:1). The mixture was heated at 110 °C for 0.5−1 h and then concentrated and the solid residue was collected by filtration and washed with ethyl ether and finally recrystallized from acetonitrile. Products were characterized by NMR and melting point.[41]

Laser Flash Photolysis. Laser flash photolysis experiments were performed with a Q-switched Nd:YAG laser, Quantel Brilliant with excitation at 355 nm and a constant laser power of 70 mJ/pulse and a 150-W Xe lamp Osram XBO as the monitoring light beam. The lamp was mounted in a PTI A1010 lamp housing system and powered by a PTI LPS-220/250 power supply. The lamp beam was passed through an included water filter before impinging on the entrance of the cell holder. An electronic shutter, Uniblitz, controlled by a Model T132 Shutter Driver/Timer, both from Vincent Associates, was placed between the water filter and the cell holder. The shutter was triggered by the Q-switch out from the laser and was opened for 7 ms during each flash. Two lenses and slits were used to collimate and focus the monitoring light to the cell holder and to the entrance slit of the monochromator, PTI 01−001, with a 1200 line/mm grating and $f = 4$. A photomultiplier detector mounted in a homemade housing was fitted to the monochromator exit slit port. The photomultiplier tube was a Hamamatsu R-928, with a voltage divider wired specifically to allow for high output currents caused by the high monitoring light input.

PMT signals were monitored with a Hewlett-Packard 54540A 500 MHz, 1 Gs/s digital oscilloscope used in DC mode. Triggering for the oscilloscope was achieved by an external PTI optical beam divider trigger. The signals can be stored and averaged in the same scope at the repetition rate of the laser pulse (10 Hz) or can be fed to a personal computer equipped with a National Instruments GPIB interface and home designed software for data acquisition and treatment. Software written in National Instruments LabViews 3.0 graphical language controls the monochomator and laser firing.

The changes in intensity of the monitoring light were converted to optical density by using: $\Delta\mathbf{OD} = \mathbf{log}\ [\boldsymbol{I}^{\circ}/(\boldsymbol{I}^{\circ} - \Delta\boldsymbol{I}(\boldsymbol{t}))]$ where $\Delta I(t)$ (mV) is the observed signal and I° (mv) is the average of measured lamp intensities prior to the laser pulse. Decay times were obtained by nonlinear least-squares data reduction using a modified Levenberg−Marquardt method. Transient spectra at delay times, t_d, after the laser pulse were constructed from several decay traces over the wavelength region of interest imported to Origin-5.0 software and subsequently plotting of ΔOD vs λ.

Optimal results were obtained with solutions with absorbance 0.6 at the excitation wavelength. Solutions (3 mL) of quinoxalin-2-one, with absorbances between 0.2 and 0.6 at 355 nm were

purged with N_2 for 20 min in a 10 mm fluorescence quartz cell sealed with a septum. Immediately after purging, an aliquot of pure or diluted amine was added through the septum for the quenching experiments.

Bimolecular rate constants were obtained from slopes of Stern−Volmer type plots of $1/\tau$ vs [quencher]. For decay of an ion−radical pair, first-order rate constants were estimated from the inverse of lifetime of the monoexponential decay of the respective absorptions.

Transient spectra in the presence of amines were made typically with not more than 4 laser pulses for each monitored wavelength. When flash photolysis was made in the presence of TEA, the integrities of solutions were assured by taking 10 min rest intervals between each wavelength measurement. Also, the UV spectra of solutions were checked after a few laser shots.

Triplet Quantum Yield. Triplet quantum yield for *N*-methylquinoxalin-2-one were measured by energy transfer to β-carotene with benzophenone as standard. The measurement were made by monitoring the 520 nm ΔOD corresponding to β-carotene triplets[42] of solutions of MeNQ and benzophenone in acetonitrile, whose absorbances at 355 nm were matched aproximately to 0.2.

Aliquots of β-carotene in benzene were added to the former N_2 purged solutions to reach a plateau in the absorption signal at 520 nm, to ensure complete energy transfer to β-carotene. The triplet quantum yield was calculated by using: $\Phi^T = (\Delta OD_{MeNQ}/\Delta OD_{Bzphe})x\ \Phi^T_{Bzphe}$, where ΔOD_{MeNQ} and ΔOD_{Bzphe} represent the optical densities of β-carotene triplet at 520 nm sensitized respectively by MeNQ and benzophenone and Φ^T_{Bzphe} is the triplet quantum yield of benzophenone taken as 1.00.[43] The mean value of three measurements was $\Phi^T = 1.06 \pm 0.18$. To be sure that no direct excitation of β-carotene takes place, a cell with pure purged acetonitrile was irradiated with the same aliquots used in the preceding experiments. In this cell no absorption at 520 nm were observed indicating no direct excitation of β-carotene. The integrities of the solutions were monitored by UV spectrophotometry and no more than 4 laser pulses were used at each β-carotene concentration. This procedure assumes an energy transfer yield of 100%.

Semiempirical Quantum Mechanical Calculations. Semiempirical quantum mechanical calculations were made using a Windows version of HyperChem-6.01 by HyperCube, Inc. in a compatible personal computer with a Intel Celeron processor of 466 MHz with 64 MB of RAM. The amount of RAM precludes ZINDO/S IC calculations with more than 5 + 5 MO due to the computing time. The results obtained by including more MO (10 + 10) increase the number of absorption lines in the high-energy region beyond the range of UV spectrometers without affecting the spectrally interesting region. All spectral calculations were checked for negative frequencies, and if they were found, a new geometrical optimization was made starting by modifying the torsional angle between phenyl and heterocycle moieties.

Acknowledgment. We thank the Facultad-CEPEDEQ 2000 project for the financial support, and to Clifford Bunton for his valuable suggestions and grammatical corrections. A. Cañete thanks Universidad de Chile for a PG,53,99 Post Grade fellowship.

References and Notes

(1) Vega, A. M.; Gil, M. J.; Basilio, A.; Giraldez, A.; Fernandez-Alvarez, E. *Eur. J. Med. Chem. Chim. Ther* **1986**, *21*, 251−254.

(2) Manca, P.; Peana, A.; Savelli, F.; Mulé, A.; Pirisino G. *Il Farmaco* **1992**, *47*, 519−522.

(3) Loriga, M.; Fiore, M.; Sannaand, P.; Paglietti, G. *Il Farmaco* **1995**, *50*, 289−301.

(4) Lawrence, D. S.; Cooper, J. E.; Smith, C. D. *J. Med. Chem.* **2001**, *44*, 594−601.

(5) McQuaid, L. A; Smith, E. C. R.; South, K. K.; Mitch, C. H.; Schoepp, D. D.; True, R. A.; Calligaro, D. O.; O'Malley, P. J.; Lodge, D.; Ornstein, P. L. *J. Med. Chem*. **1992**, *35*, 3319−3324.

(6) Hara, S.; Yamagushi, M.; Nakamura, M.; Ohkura, Y. *Chem. Pharm. Bull*. **1985**, *33*, 3493−3498.

(7) Iwata, T.; Yamagushi, M.; Hara, S.; Nakamura, M.; Ohkura, Y. *J. Chromatogr*. **1986**, *362*, 209−216.

(8) Nakashima, K.; Okamoto, M.; Yoshida, K.; Kuroda, N.; Akiyama, S.; Yamagushi M. *J. Chromatogr*. **1992**, *584*, 275−279.

(9) Yamagushi, M.; Iwata, T.; Inoue, K.; Hara, S.; Nakamura, M. *Analyst* **1990**, *115*, 1363−1366.

(10) Sandmann, B. W.; Grayeski ,M. L. *J. Chromatogr. B Biomed. Appl*. **1994**, *635*, 123−130.

(11) Bourson, J.; Pouget, J.; Valeur, B. *J. Phys. Chem*. **1993**, *97*, 4552−4557.

(12) Ahmad, A. R.; Mehta, L. K.; Parrick, J. *Tetrahedron* **1995**, *51*, 12 899−12 910.

(13) Nishio, T. *J. Chem. Soc., Perkin Trans. 1* **1990**, 565−570.

(14) De la Fuente, J. R.; Cañete, A.; Zanocco, A. L.; Saitz, C.; Jullian, C. *J. Org. Chem.* **2000**, *65*, 7949−7958.

(15) Ci, X.; da Silva, R. S.; Nicodem, D.; Whitten, D. G. *J. Am. Chem. Soc*. **1989**, *111*, 1337−1343.

(16) Gan, H.; Whitten, D. G. *J. Am. Chem. Soc*. **1993**, *115*, 8031−8037.

(17) Schanze, K. S.; Lee, L. Y. C.; Giannotti, C.; Whitten, D. G. *J. Am. Chem. Soc*. **1986**, *108*, 2646−2655.

(18) Gan, F.; Zhao, X.; Whitten, D. G. *J. Am. Chem. Soc.* **1991**, *113*, 9409−9411.

(19) Yokoyama, Y.; Hayata, H.; Ito, H.; Kurita, Y. *Bull. Chem. Soc. Jpn.* **1990**, *63*, 1607−1610.

(20) Jones, G., II; Lu, L. N. *J. Org. Chem*. **1998**, *63*, 8938−8945.

(21) Jonsson, M.; Wayner, D. D. M.; Lusztyk, J. *J. Phys. Chem.* **1996**, *100*, 17 539−17 543.

(22) Liu, W. Z.; Bordwell, F. G. *J. Org. Chem*. **1996**, *61*, 4778−4783.

(23) Clennan, E. L.; Noe, L. J.; Wen, T.; Szneler, E. *J. Org. Chem.* **1989**, *54*, 3581−3584.

(24) Cohen, S. G.; Davies, G. A.; Clark, W. D. K. *J. Am. Chem. Soc.* **1972**, *94*, 869−874.

(25) Hu, K.; Evans, D. H. *J. Phys. Chem.* **1996**, *100*, 3030−3036.

(26) Pause, L.; Robert, M.; Savéant, J. M. *J. Am Chem. Soc.* **2001**, *123*, 4886−4895.

(27) Lewis, F. D.; Cohen, B. E. *J. Phys. Chem.* **1994**, *98*, 10 591−10 597.

(28) Burkhart, R. D.; Jhon, N−I. *J. Phys. Chem.* **1991**, *95*, 7189−7196.

(29) Kiyota, T.; Yamaji M.; Shisuka, H. *J. Phys. Chem.* **1996**, *100*, 672−679.

(30) Oyama, M.; Nozaki, K.; Okasaki, S. *Anal. Chem.* **1991**, *63*, 1387−1392.

(31) Peters, K. S.; Cashin, A.; Timbers, P. *J. Am. Chem. Soc.* **2000**, *122*, 107−113.

(32) Deward, M. J. S.; Zoebisch, E. G.; Healy, E. F.; Stewart, J. J. P. *J. Am. Chem. Soc.* **1985**, *107*, 3902−3909.

(33) Stewart, J. J. P. MOPAC: A Semiempirical Molecular Orbital Program. *J. Comput. Aid. Mol. Des.* **1990**, 4: 1−105.

(34) Gao, G.; Wei, C. C.; Jeevarajan, A. S.; Kispert, L. D. *J. Phys. Chem.* **1996**, *100*, 5362−5366.

(35) Hu, K.; Evans, D. H. *J. Phys. Chem.* **1996**, *100*, 3030−3036.

(36) Allinger, N. L. *J. Am. Chem. Soc.* **1977**, *99*, 8127−8134.

(37) Ridley, J. E.; Zerner, M. C. *Theor. Chim. Acta* **1973**, *32*, 111−134.

(38) Forber, C.; Kelusky, E. C.; Bunce, N. J.; Zerner, M. C. *J. Am. Chem. Soc*. **1985**, *107*, 5884−5890.

(39) *HyperChem Computational Chemistry, Part 2, Theories and Methods, Hypercube Inc.*, 1996, Chapter 12, and references therein.

(40) LaChapelle, M.; Belletête, M.; Poulin, M.; Godbout, N.; LeGrand, F.; Héroux, A.; Brisse, F. *J. Phys. Chem.* **1991**, *95*, 9764−9772.

(41) Nishio, T. *J. Org. Chem*. **1984**, *49*, 827−832.

(42) Bensasson, R. V.; Dawe, E. A.; Long, D. A.; Land, E. J. *J. Chem. Soc. Faraday Trans. 1* **1977**, *73*, 1319−1325.

(43) Murov, S. L.; Carmichael, I.; Hug, G. L. In *Handbook of Photochemistry*; Marcel Dekker: New York, 1993; Vol 1, p 378.